



Case Study

Design for Metal Additive Manufacturing – Part 1: Materials Selection and Process Parameter Optimization

Developed and curated by the Ansys Academic Development Team

Navid Manai and János Plocher

education@ansys.com

Summary

As one of the pillars of Industry 4.0, additive manufacturing (AM) is finding its place in engineering education curricula. The standard industry practice utilizes AM simulation to ensure that components are produced with minimal experimental trial and error. And this case study begins to explore this AM workflow in the context of producing an aeronautics bracket through Metal Additive Manufacturing (MAM). This workflow starts from material selection in Ansys Granta EduPack and progresses to optimizing the processing parameters used in MAM for this selected material to ensure minimal porosity. For this, the tools available in the Ansys Additive software are utilized.

Table of Contents

1. Introduction.....	3
1.1 Background.....	3
2. Material Selection	4
3. Processing Parameter Optimization	6
3.1 Experimental Testing	6
3.2 Single Bead Simulation	7
3.3 Porosity Parametric Simulation	10
4. Conclusions and Further Analysis.....	12

1. Introduction

1.1 Background

Different types of brackets can be found in various sections of an airplane. Weight plays a critical role in the design of such airplane components. Thus, today's airplanes are commonly built from lightweight composite materials and high-performance alloys. Utilizing materials with a high stiffness and strength to weight ratio is one key aspect in aircraft design, however, the geometry of the components also contributes significantly to the specific performance. In this case study we will consider that the bracket will be fabricated using additive manufacturing (AM), due to its potential for reducing the component's weight.

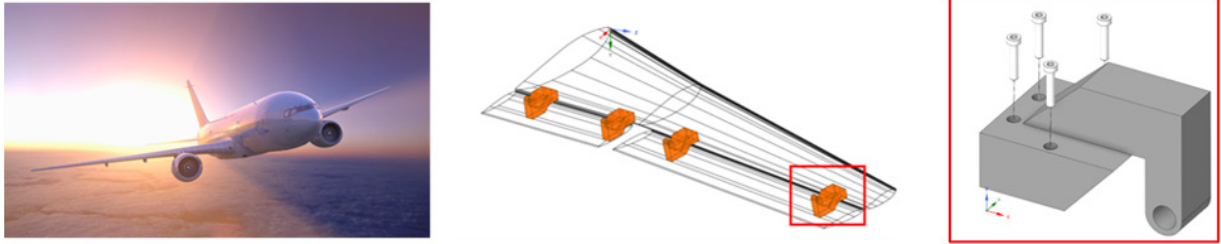


Figure 1: Airplane flap bearing bracket example (not to scale).

The case study is split into three parts, as shown in Table 1, following the design for AM (DfAM) workflow (see Figure 2). The objective of this first part of the case study is to (i) find the appropriate material that satisfies the structural requirements (function, objective and constraints associated with the bracket) and to (ii) identify the optimized processing parameters that will be used in additive manufacturing of the component discussed in this case study.

Table 1: Division of the metal additive manufacturing case study in parts.

Part	Content	Software	Hyperlink
1	<ul style="list-style-type: none">Strategic Materials SelectionLPBF process parameters optimization	<ul style="list-style-type: none">Ansys Granta EduPackAnsys Additive Suite	Current document
2	<ul style="list-style-type: none">Topology optimizationBuild preparation (orientation, support structures, <i>etc.</i>)	<ul style="list-style-type: none">Ansys DiscoveryAnsys SpaceClaim	Find case study here
3	<ul style="list-style-type: none">Stress and distortion analysis in LPBF	<ul style="list-style-type: none">Ansys AdditiveSuite	Find case study here

In subsequent parts of the case study, the part geometry will be topologically optimized to reduce weight. Once the optimization has been solved, outputs like stress, strain and displacement will be evaluated. Then, the build setup is defined where the part orientation on the baseplate and the support structure are identified. Prior to the physical printing of the part, in the third step, the laser powder bed fusion (LPBF) process is simulated to analyze the stress and distortion that can occur within the AM process and check if there may be possible issues with the build process as a result.

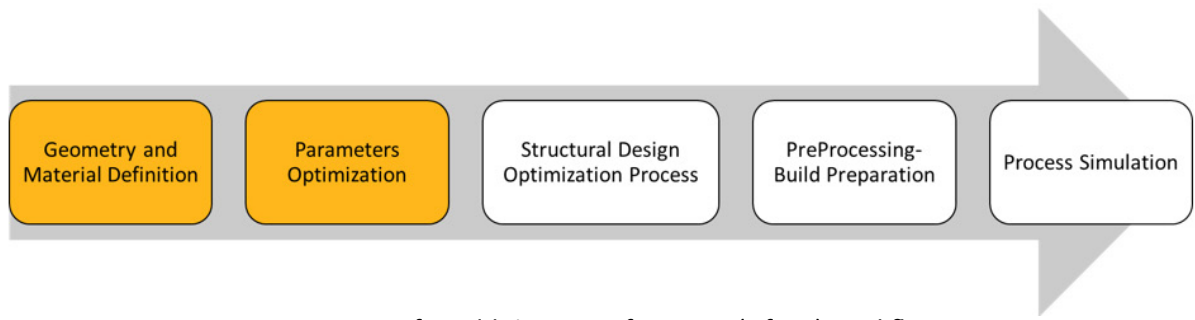


Figure 2: Design for additive manufacturing (DfAM) workflow.

2. Material Selection

In order to find suitable materials for this bracket, the Ashby systematic material selection methodology will be used, for which the design requirements can be identified as shown in Table 2.

Table 2: Design requirements following Ashby's methodology for a systematic material selection

Function	Beam in Bending
	Stiffness-limited design
Constraints	Minimum Young's Modulus: 50 GPa
	Minimum Yield strength: 150 MPa
	Stress corrosion cracking resistance: Slight susceptible or not susceptible
	Manufactured with Selective Laser Melting
Objective	Lightweighting (minimize mass and maximizing stiffness)

When assembled, the bracket will be bolted to the wing on one side and connected to a flap on its other side. When the flaps are down, such as during take-off (to create lift) and descending (to create drag), the bracket will experience a significant force produced by the air pressure on the flap. This causes the bracket to experience a bending moment. Since controlling the amount of deflection resulting from this stress is desirable, we can simplify the load conditions and consider the function of the bracket to be a beam in bending in a stiffness-limited design.

Next, we consider the constraints for this bracket. The minimum mechanical properties listed in Table 2 are determined based on the loading condition that the component will be experiencing. Furthermore, the bracket will operate in a high moisture environment, so the material needs some level of stress corrosion cracking resistance. As previously discussed, additive manufacturing of the component is desirable, since it provides the freedom in design of the bracket's geometry. Here, the assumption is that the manufacturer has selective laser melting (SLM) machines available for production of these components and hence, materials that are compatible with the SLM process must be considered in this material selection project.

The Aerospace materials subset in the Level 3 Aerospace database in [Ansys Granta EduPack](#) will be used for this selection to allow for all properties of interest to be considered. After applying the constraints

by using the Limit and Tree stages, a Chart can be created to compare the remaining 151 materials (out of the initial 803) visually, in regards to their Density and Young's Modulus. Using the [performance index booklet](#), we can identify the performance index for a beam in bending in a stiffness-limited design: $E^{1/2}/\rho$.

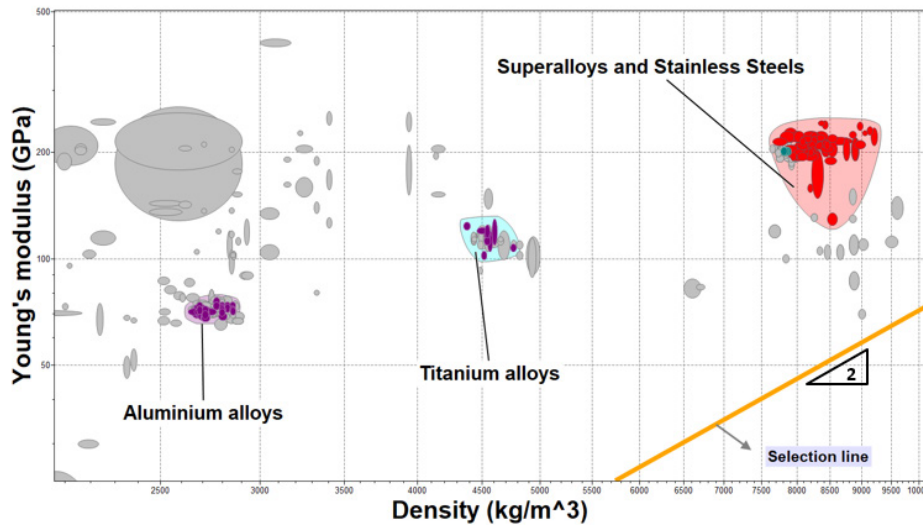


Figure 3: Ashby map of Young's modulus versus material density of aerospace materials as created by Ansys Granta EduPack. It includes a selection line of slope 2, indicating materials with the same specific stiffness for a beam in bending loading case.

On this chart (see Figure 3), 3 clusters of materials can be identified which have passed the selection stages at this point, namely, Steels and Superalloys, Titanium alloys and Aluminum alloys. To identify the best performing materials for this application, a selection line with a slope of 2 (determined by the material performance index) can be used. Upon moving this line towards the top left corner of the chart, materials with larger density and lower stiffness will gradually be eliminated from the selection pool.

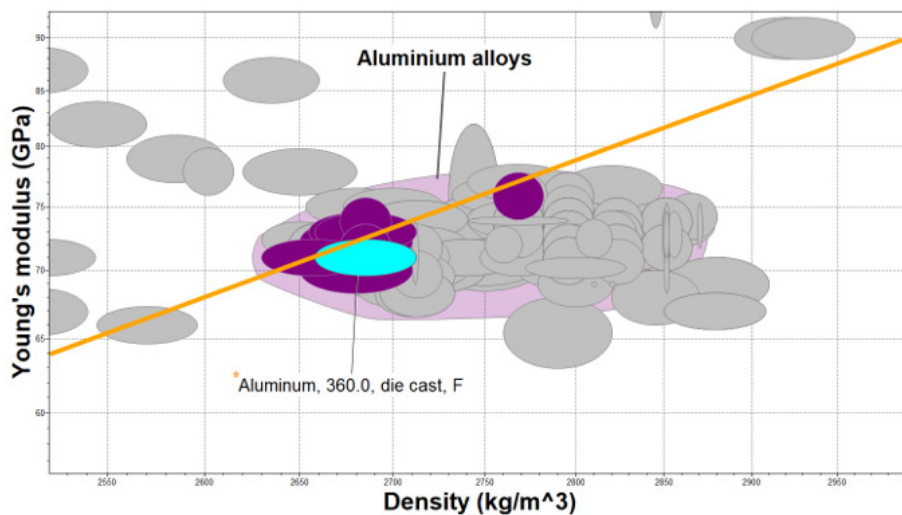


Figure 4: Ashby map of Young's modulus versus material density, as created by Ansys Granta EduPack, showing that by moving the selection line aluminum alloys perform the best for the function under consideration.

By doing so, a group of Aluminum alloys are shown to be best performing (see Figure 4). Aluminum 360 (also known as AlSi10Mg) can be chosen as the final choice for this bracket, as this alloy is one of the most-commonly researched, tested and hence used materials in additive manufacturing with SLM.

3. Processing Parameter Optimization

In metal additive manufacturing, one of the first challenges that engineers need to tackle is identifying the appropriate processing parameters with which components with minimal or no defects can be produced. More specifically in powder bed fusion (PBF) processes, there are different types of defects that can occur in 3D-printed components; however, they can be mostly categorized into porosities and cracking. For this case study, eliminating the possibility of porosity generation will be the focus.

3.1 Experimental Testing

Traditionally, experimental testing is used to optimize the PBF processing parameters. The first step is to melt single tracks on the powder bed (e.g. by using different laser power and laser speed values for each melt track, in the case of SLM) and characterize the topology/size of the melt pool. Using these results, a processing map (see Figure 5) is created which shows if using each parameter set would result in different types of porosity. This map can also determine which parameter sets would result in sufficient penetration (not too much to create keyholing porosity and not too low to create lack of fusion porosity or balling), maximizing the possibility of producing components with minimal porosity. These parameter sets are typically identified as belonging to the processing window of the material.

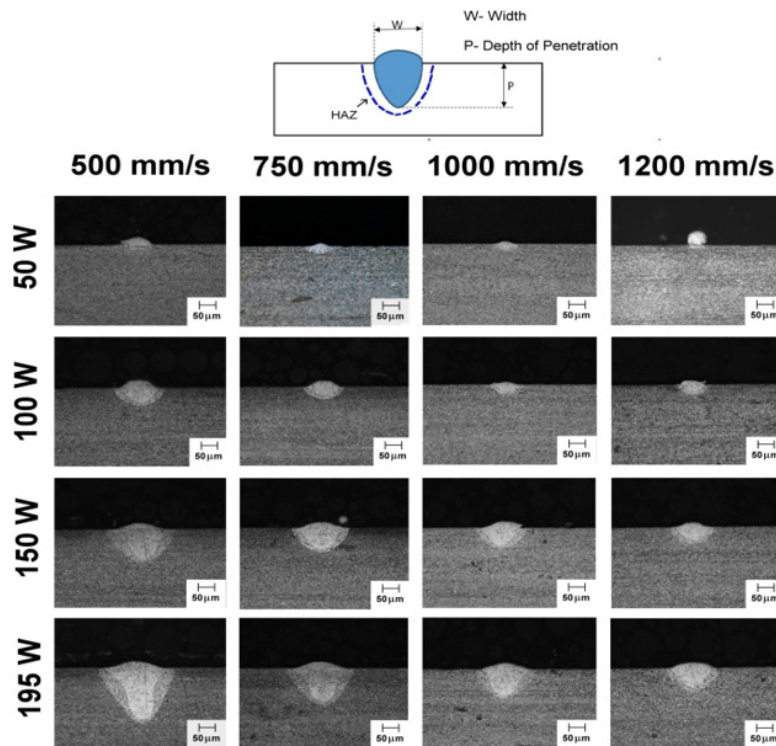


Figure 5: Micrographs of the heat-affected zones (HAZs) for single track SLM prints as a function of laser power and print speed¹.

¹ Figure adapted from Dilip, J.J.S., Zhang, S., Teng, C. et al. Influence of processing parameters on the evolution of melt pool, porosity, and microstructures in Ti-6Al-4V alloy parts fabricated by selective laser melting. Prog Addit Manuf 2, 157–167 (2017). <https://doi.org/10.1007/s40964-017-0030-2>

The second step is to confirm the results of the first step and further narrow down the processing window, by utilizing the parameter sets that create sufficient penetration to 3D-print small cubes. Each cube is then characterized to determine its solid density (100% - porosity%). The parameter set(s) that create the highest solid density are hence chosen as the optimal processing parameters for additive manufacturing of the metallic alloy in question (cracking defects are also considered at both steps). It is clear that running these experimental tests can be time-consuming and expensive. Simulation is often used beforehand to narrow down the scale of these Design of Experiments tests. For this case study, both the above-mentioned steps can be carried out for the selected material, AlSi10Mg (Aluminum 360), using the thermal solver operating within the Additive Science simulation tool, available in the Ansys Additive software.

3.2 Single Bead Simulation

Using the Single Bead simulation available as part of the Additive Science tool, simulation of melting single tracks on the powder bed will be carried out. The range of processing parameters explored for this stage can be seen in Figure 6.

Configure Single Bead Parametric Simulation
Configured Permutations: 108 out of 300 maximum permutations

Details

Simulation Title *
Single Bead Simulation - AlSi10Mg

Tags
Case Study X Airplane Bracket X AlSi10Mg X Melt Pool Size X + Tag

Tag your project for efficient filtering, grouping, and reporting

Description
Processing parameter optimisation for SLM of AlSi10Mg by using melt pool characterisation

Number of Cores
4

Material Configuration

Material *
AlSi10Mg

Machine Configuration

Machine
Generic

Baseplate Temperature (°C) *
80

☐ Use Characteristic Width Calculation Mode ⓘ

Bead Type
Bead on powder layer

Layer Thickness (µm) *
50

Laser Beam Diameter (µm) *
80

Laser Power (W) *
200 X 225 X 250 X 275 X 300 X 325 X 350 X 375 X 400 X

Scan Speed (mm.s⁻¹) *
400 X 500 X 600 X 700 X 800 X 900 X 1,000 X 1,100 X 1,200 X 1,300 X 1,400 X
1,500 X

Each value has a recommended range between 500 and 2500. See Additive User's Guide for more information.

Geometry Configuration

Bead Length (mm) *
3

Total Permutations: 108 individual permutations selected

Save Start Duplicate Export Delete

Figure 6: Processing parameters used as input for the single bead parametric simulation (Ansys Additive user interface).

Baseplate Temperature refers to the temperature of the baseplate on to which the layer of powder being melted is distributed. The Bead Type selected determines if the tracks are melted on a layer of powder (in case of Bead on powder layer) or directly on solid material (in case of Bead on baseplate). This setting affects the calculation of material state, which in turn affects the material properties used in the solving process, as well as in the laser flux model. Layer Thickness refers to the thickness of the powder layer coating that is applied with every pass of the recoater blade. Laser Beam Diameter is the width of the laser on the powder or substrate surface defined using the $D4\sigma$ beam diameter definition (second moment width, calculated to be four times the standard deviation of the vertical and horizontal distribution intensity σ). Usually, this value is provided by the machine manufacturer and is sometimes called laser spot diameter. A schematic of these terms in a machine setup can be seen in Figure 7.

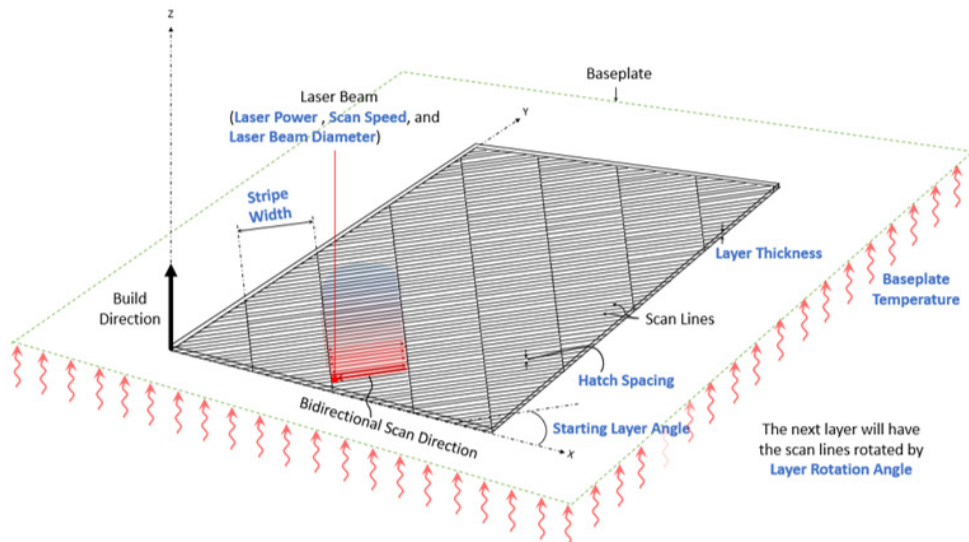


Figure 7: Machine parameters for a typical rotating stripe scan pattern.

Within each permutation (simulation of the melt track created by using a set of processing parameters), the laser beam would melt a line on the powder bed, whose length is dictated by the Bead Length identified as input (see Figure 8).

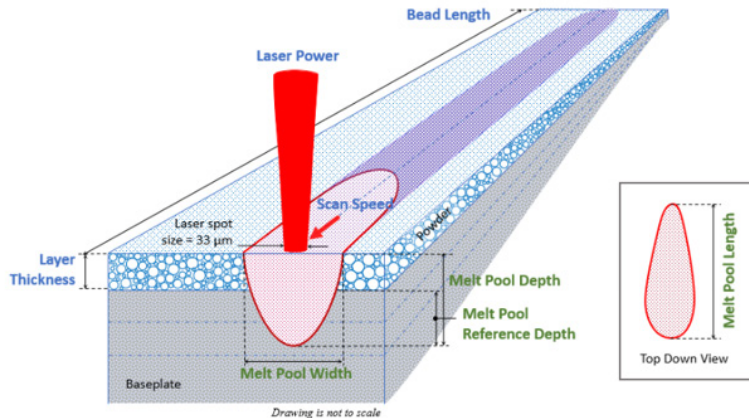


Figure 8: Schematic of single bead scan on powder showing the melt pool dimensions. Labels in blue denote inputs, whereas green labels represent outputs.

Upon completion of all permutations, the widths, depth and length of the resulting melt pools can be found in and exported from the “Completed Simulation” section of the Dashboard, within the “Output Files” and under “Single Bead Summery” (see Table 3). When exploring this spreadsheet, the median values would be of interest, since the average values are more affected by the smaller melt pool sizes forming at the start of the melting process.

Table 3: Example subset of results from single bead simulation, providing average and median melt pool sizes as a function of laser power and scan speed. Median values are highlighted in gold.

Laser Power (W)	Scan Speed (mm/s)	Average Melt Pool Reference Depth (mm)	Average Melt Pool Length (mm)	Average Melt Pool Reference Width (mm)	Median Melt Pool Reference Depth (mm)	Median Melt Pool Length (mm)	Median Melt Pool Reference Width (mm)
400	1000	0.231	0.428	0.267	0.235	0.459	0.276
250	500	0.17	0.33	0.255	0.175	0.343	0.264
300	700	0.187	0.364	0.256	0.192	0.383	0.265
250	1500	0.036	0.258	0.135	0.037	0.264	0.138
300	1400	0.076	0.32	0.181	0.078	0.333	0.186
325	1300	0.101	0.351	0.206	0.104	0.368	0.212
275	1000	0.099	0.303	0.204	0.101	0.313	0.21
325	1400	0.091	0.349	0.197	0.094	0.366	0.203
275	1300	0.067	0.293	0.174	0.069	0.303	0.178
325	600	0.26	0.395	0.285	0.265	0.42	0.296
400	1500	0.131	0.42	0.223	0.134	0.449	0.23
400	1400	0.148	0.421	0.23	0.151	0.449	0.237
400	900	0.264	0.429	0.275	0.268	0.461	0.286
225	900	0.067	0.244	0.171	0.069	0.249	0.175
200	900	0.044	0.21	0.142	0.046	0.213	0.146

In order to investigate this data, a set of criteria is required which would link melt pool sizes with the likelihood in generation of different types of porosity. An experimentally-defined example of these criteria can be expressed as:

- To avoid Lack of Fusion porosity: melt pool depth > 2.5 layer thickness
- To avoid Keyholing porosity: melt pool depth-to-width ratio < 0.95
- To avoid Balling: melt pool length-to-width ratio < 4.0

A visual map can be created by applying these criteria to the melt pool sizes simulated for these sets of processing parameters (see Figure 9). It can be clearly observed that when laser power is low and/or laser speed is high, the possibility of generation of Lack of Fusion porosity increases (the red section). This is because sufficient heat would not be available to penetrate the powder bed and hence the melt pool depth would be small, which would in turn increase the possibility of powder particles remaining unmelted between consecutive layers.

However, within the range of the SLM parameter values explored, there seems to be no possibility of keyholing or balling occurring within the AM process. On the other hand, the green section of the map refers to a preliminary processing window which satisfies all the above-mentioned criteria; these processing parameter sets will be a good starting point for the next step, in which the possibility of porosity generation in components will be further investigated and the processing window can be narrowed down accordingly. It is also worth mentioning that this processing map is material dependent and must be verified through experiments.

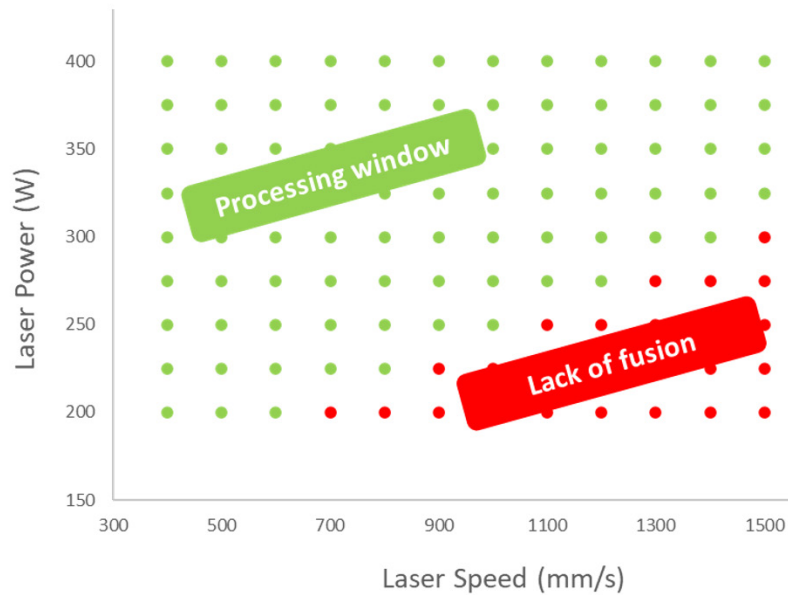


Figure 9: AlSi10Mg processing map (created with simulated meltpool sizes), highlighting the acceptable processing window and Lack of Fusion possibility for this material when manufactured with SLM, using the processing parameters identified in Figure 6.

3.3 Porosity Parametric Simulation

Following the previous step, 3D-printing of small cubes would be simulated, using the processing window identified previously. For this, the Porosity Simulation capability available within the Additive Science tool will be utilized which makes use of the same thermal solver discussed before, however instead of simulating single melt tracks, creating bulk cubes will be the focus.

This means that a few extra processing parameters would be involved at this step, namely, Hatch Spacing (the distance between tracks melted at each layer), Starting Layer Angle (orientation of fill rasters on the first layer of the part. This is measured from the X axis, such that 0 degrees results in scan lines parallel to the X axis), Layer Rotation Angle (the angle at which the major scan vector orientation changes from layer to layer, commonly 67 degrees) and Slicing Stripe Width (When using the stripe pattern for scan strategy, the geometry can be broken up into sections, called stripes. The stripes are scanned sequentially to break up what would otherwise be very long continuous scan vectors. Slicing Stripe Width is commonly set to 10 mm wide).

To run this step, 34 cubes ($1 \times 1 \times 1 \text{ mm}^3$) will be simulated using the range of parameters shown below (taken from the processing window in Figure 9):

- Laser Power: 200 – 400 W (steps of 25 W)
- Laser Speed: 400 – 1400 mm/s (steps of 100 mm/s)
- Beam Diameter: 80 μm
- Layer Thickness: 50 μm
- Hatch Spacing: 0.1 – 0.25 μm (steps of 0.05 μm)
- Baseplate Temp: 80 $^{\circ}\text{C}$
- Rotation Angle: 67 $^{\circ}$

With this input, the resulting Solid Ratio (defined as 1-volume fraction of pores) for each cube (simulated with each set of processing parameters), would be available as shown in Table 4.

Table 4: Example subset of results from the Porosity Simulation, showing the Solid Ratio of cubes printed when using the defined processing parameters. The optimum set of parameters is highlighted in gold.

Geometry Height (mm)	Geometry Length (mm)	Geometry Width (mm)	Starting Layer Angle (deg)	Layer Rotation Angle (deg)	Laser Power (W)	Scan Speed (mm/s)	Layer Thickness (mm)	Hatch Spacing (mm)	Slicing Stripe Width (mm)	Void Ratio	Powder Ratio	Solid Ratio
1	1	1	0	67	200	1000	0.05	0.2	10	0	0.0909	0.9091
1	1	1	0	67	200	800	0.05	0.25	10	0	0.0687	0.9313
1	1	1	0	67	200	1200	0.05	0.15	10	0	0.0552	0.9448
1	1	1	0	67	200	1400	0.05	0.1	10	0	0.0326	0.9674
1	1	1	0	67	200	800	0.05	0.2	10	0	0.0247	0.9753
1	1	1	0	67	200	1000	0.05	0.15	10	0	0.0057	0.9943
1	1	1	0	67	200	600	0.05	0.2	10	0	0.0004	0.9996
1	1	1	0	67	400	1400	0.05	0.2	10	0	0	1
1	1	1	0	67	300	1000	0.05	0.2	10	0	0	1
1	1	1	0	67	200	1200	0.05	0.1	10	0	0	1
1	1	1	0	67	400	1200	0.05	0.2	10	0	0	1

To visualize this data better, the energy density used for each cube is calculated, using the equation below:

$$\text{Energy Density (J/mm}^2\text{)} = \text{Laser Power} / (\text{Laser Speed} \times \text{Hatch Spacing})$$

This is a good representation of the heat flux transferred to the material at each point in time and when calculated for each set of processing parameters used to build the above-mentioned small cubes, it can be a suitable tool in predicting whether the final microstructure of the component may have porosity and how much, as shown in Figure 10.

Depending on the application, the threshold for an acceptable level of porosity in AM components can vary. Here, a Solid Ratio of 95% has been chosen as the threshold. This means that the processing parameters that would result in a smaller Solid Ratio are unacceptable as the resulting microstructure would include a larger than acceptable volume fraction of Lack of Fusion porosity (this is the only type of porosity that the Porosity Simulation capability models). Therefore, the optimum set of processing parameters can be defined as the one that correlates to the smallest energy density value which can yield a Solid Ratio of 100% or as close as possible to this (the orange dot in Figure 10). The fact that the Porosity Simulation capability only models Lack of Fusion porosity means that although larger values of energy density seem to yield a complete lack of porosity, but there would be an increased risk of Keyholing developing in the microstructure, hence the blue section in Figure 10 is best to be avoided.

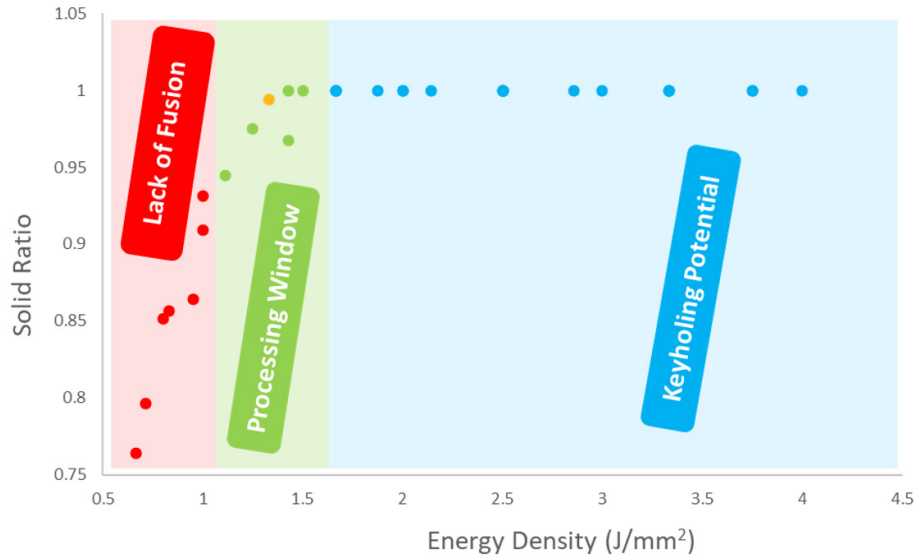


Figure 10: Plot of solid ratio versus energy density highlighting the ideal processing window alongside energy density realms which lead to a lack of fusion and high porosity as well as keyholing and low porosity.

So, the set of processing parameters chosen to manufacture this Bracket are as follows:

Table 5: List of processing parameters chosen to be used in MAM of the flap-bearing bracket, some of which were optimized using the Single Bead and Porosity simulations in Ansys Additive (i.e., Laser Power, Laser Speed and Hatch Spacing)

Material	Laser Power	Laser Speed	Hatch Spacing	Layer Thickness	Scan Pattern	Beam Diameter	Baseplate Temperature
AlSi10Mg	200 W	1000 m/s	0.15 mm	0.08 mm	Stripe -67°	0.08 mm	80°C

4. Conclusions and Further Analysis

This study has elucidated the strategic material selection for a flap bearing of an aircraft intended for SLM printing, using Ansys Granta EduPack as well as processing parameters optimization using Ansys Additive. Using Granta EduPack, Aluminum 360 (also known as AlSi10Mg) was identified as the suitable material candidate under consideration of the functions, constraints, and objective for the component under investigation. The process parameter optimization focused on the single bead simulation and porosity predication based upon a range of different process parameters. The method of deriving the ideal processing windows were highlighted by showcasing its relationship with the laser speed and power as well the laser's energy density.

The findings of these simulation can help in further analysis of the LPBF workflow. In the second part of the case study, we will explore lightweighting of this bracket through topology optimization in which we will assign AlSi10Mg as the material for this component. And in the third and final part, we will simulate the LPBF process to investigate the stresses and distortions that can develop during the build, when the parameters identified in Table 5 are utilized in MAM of this flap-bearing bracket. It is however important to mention that the above analysis was performed with various assumptions and simplifications. For example, the Porosity Simulation does not model Balling porosity which can be a significant problem in LPBF of certain alloys (including some aluminum alloys). So, it is crucial that the results of these simulations are validated against experimental data.

© 2023 ANSYS, Inc. All rights reserved.

Use and Reproduction

The content used in this resource may only be used or reproduced for teaching purposes; and any commercial use is strictly prohibited.

Document Information

This case study is part of a set of teaching resources to help introduce students to multiphysics topics.

Ansyes Education Resources

To access more undergraduate education resources, including lecture presentations with notes, exercises with worked solutions, MicroProjects, real life examples and more, visit www.ansys.com/education-resources.

Feedback

If you notice any errors in this resource or need to get in contact with the authors, please email us at education@ansys.com.

ANSYS, Inc.
Southpointe
2600 Ansys Drive
Canonsburg, PA 15317
U.S.A.
724.746.3304
ansysinfo@ansys.com

If you've ever seen a rocket launch, flown on an airplane, driven a car, used a computer, touched a mobile device, crossed a bridge or put on wearable technology, chances are you've used a product where Ansys software played a critical role in its creation. Ansys is the global leader in engineering simulation. We help the world's most innovative companies deliver radically better products to their customers. By offering the best and broadest portfolio of engineering simulation software, we help them solve the most complex design challenges and engineer products limited only by imagination.

visit www.ansys.com for more information

Any and all ANSYS, Inc. brand, product, service and feature names, logos and slogans are registered trademarks or trademarks of ANSYS, Inc. or its subsidiaries in the United States or other countries. All other brand, product, service and feature names or trademarks are the property of their respective owners.

© 2023 ANSYS, Inc. All Rights Reserved.